Topological Analysis of an Air Flow Subjected to Electric Field

Tossaphorn Klinmalee[*1)] and Chainarong Chaktranond,[2)]

[*1)]Department of Mechanical Engineering, Faculty of Engineering, Thammasat University, Pathumthani 12120, Thailand

[2)]Department of Mechanical Engineering, Faculty of Engineering, Thammasat University, Pathumthani 12120, Thailand

Abstract

This research numerically investigates the characteristics of electric field and electrically-driven airflow. In simulations, electrode wires are installed normal to flow direction and two ground wires are placed along the side walls of a square duct. Effects of position and number of the electrodes on flow are explored. Additionally, inlet airflow velocity and applied electrical voltage are tested at 0.33 m/s and 20 kV, respectively. It is clearly observed from the numerical results that electric fields are not uniform in any planes and are high strength around electrode ends, especially at the electrodes near the ground wires. Increasing the number of electrode wires conducts the maximum strength of electric field at electrode ends to be much higher. As a result, air velocity in spanwise direction is non-uniform and high velocity appears near the electrode end close to the ground. Adjusting the electrode positions in flow direction causes the circulating flow to occur nearer the target position.

Keywords: Air Flow, High Voltage Electric Fields, Electrohydrodynamics.

1. Introduction

Hot-air drying method is widely used to preserve agricultural products and to improve the quality of materials, e.g. ceramic and wood. Due to the effects of the boundary layer or flow separation [1-3], the heat transfer on material surface is suppressed. As a result, drying period and energy consumption are much higher.

Flow manipulation by utilizing electric field is an interesting method to enhance drying efficiency because there are no moving parts and also it is able to control the drying temperature [1]. The ideal of this method is to control the air motion by utilizing the high electrical voltage. The ionized air performed by electric force is moved faster from the electrode towards the ground, and this leads to the momentum transfer between the air particles. Simultaneously, with the influence of the velocity difference between the air flow layers or shear flow, vortices are generated. This causes the moisture and heat transfer on the surface of porous materials to enhance considerably [1-4].

Chaktranond and Rattanedecho [1] experimentally explore the hot air drying combined with electric fields to enhance the moisture removal and heat transfer of packed bed, which is used for porous material. Moreover, the effects of different porosity layers on drying are examined. It is found that when the electrical voltage is applied, air streams rotate around the ground wire. This causes a high amount of heat transfer onto the material surface, resulting in the enhancement of drying rate. Additionally, the arrangement of different porosity layers affects the capillary pressure the material, and also significantly influences the drying rate.

Lai and Lai [5] enhance the drying by installing copper electrode wire above packed bed and placing ground plates above and under packed bed, respectively. The experimental results show that the rate of drying depends on the magnitudes of applied voltage and the inlet wind velocity. Lai and Wang [6] are found that applying a heat source under the packed bed can enhance drying rate. Moreover, influence of corona wind has high effectiveness when high moisture content is in packed bed or is in early period of drying process.

Ahmedou and Havet [7] apply the two-dimensional channel-flow simulations to investigate the enhancement of heat transfer by electric field. In simulations, electrode wire is as a point. In addition, electrode is in the middle of the channel, while the ground electrode is put along the lower wall applied with heat flux. The results show that when the Reynolds number of air flow is low the corona wind can increases the convective heat transfer coefficient by 3 times that of the non-electric field.

Saenewong Na Ayuttaya et al. [8] investigate air flow under the electric fields with two-dimensional simulation in which electrode and ground are assumed as small circles. The results show that the air velocity driven by the electric forces varies inversely with the distance between the electrode and the ground.

Ghassem Heidarinejad and Reza Babaei [9] perform the large eddy simulations to investigate the enhancement of water evaporation by electric fields, so-called electrohydrodynamics (EHD). The results show that the rate of water evaporation is higher with applying electric field. Moreover, the effect of EHD is suppressed when Reynolds number is higher.

From mentioned above, details of flow subjected electric fields are lack in the spanwise direction. This research applies three-dimensional simulations to investigate the electric field distribution and flow patterns of electrically-driven swirling flow by following the experiments done by Nuknan et al. [10].

2. Simulations

We consider an experiment of drying enhanced electrically-driven swirling flow done by Nuknan et al. [10], as shown in Figure 1. The dimensions of rectangular channel are 1.2 m long × 0.3 m wide × 0.3 m high. In present simulations, electrode is assumed as a point, while two ground wires are assumed as lines and put along the side walls. The velocity of air in the channel is obtained by computing the continuity and Navier-Stokes equations, as shown in Eq.(1) and (2), where last term is body force term from electric force. Three-dimensional incompressible laminar flow simulations is computed by giving the inlet uniform velocity of 0.33 m/s. The pressure at the outlet is atmospheric pressure (P_0=101 kPa) and no viscous stress is used, as well as, no-slip condition on walls,

$$\nabla \cdot \vec{u} = 0 \tag{1}$$

$$\rho\left(\frac{\partial \vec{u}}{\partial t} + (\vec{u} \cdot \nabla)\vec{u}\right) = -\nabla \vec{p} + \mu \nabla^2 \vec{u} + \vec{F}_{ee} \tag{2}$$

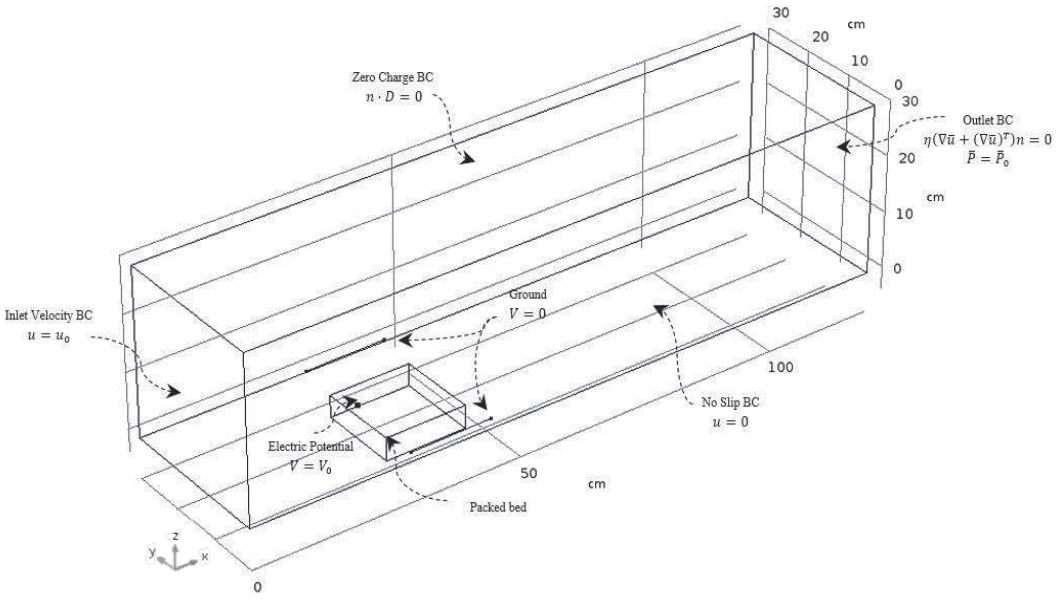

Figure 1 The computational domain and the boundary conditions

where $\vec{u}$ is velocity, t is time, $\vec{p}$ is pressure, ρ is density (1.06 kg/m^3), μ is viscosity (19.99×10^{-6} Pa.s), and $\vec{F}_{ee}$ is body force term done by electric force.

By assuming constant properties of air and electric fields, the electric force per unit volume $\vec{F}_{ee}$ performing on fluid flow is computed from electrophoretic force or Coulomb force resulting from the net uncharged within the fluid or ions injected from the electrodes,

$$\vec{F}_{ee} = q\vec{E} \tag{3}$$

where q is the space charge density can calculate with commercial software and $\vec{E}$ is the strenght of electric field.

Additionally, the electric field strenght is computed through the Maxwell equations,

$$q = \nabla \cdot \varepsilon \vec{E} \tag{4}$$

$$\vec{E} = -\nabla V \tag{5}$$

where ε is the permittivity of air (8.85522 × 10^{-12} F/m) and V is the electric potential at electrode. In the simulations, the boundary condition solving electric field, as shown in Figure 1, are considered as zero charge symmetry. Electrical voltage at electrode and ground positions are V = 20 kV and V = 0, respectively

The computational scheme uses a finite element method of tetrahedral and a collocation grid. Due to limitation of CPU and machine memory, the number of elements is approximately 100,000 elements, however, it is enough for these simulations. The governing equations are solved by using COMSOL Muliphysics 4.4.

3. Results and discussion

3.1 Electric field distribution

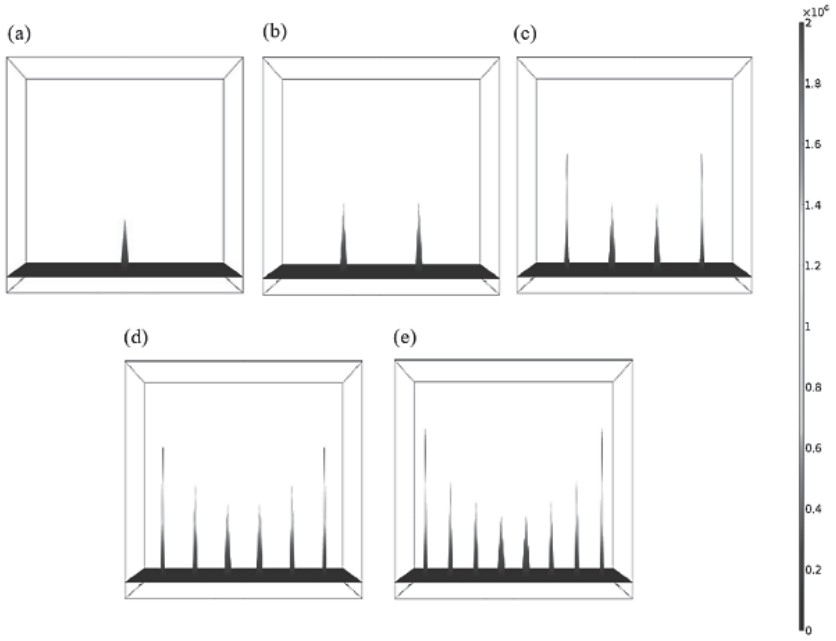

Figure 2 Electric fields (V/m) in various the number (n) of electrodes: (a) n = 1, (b) n = 2, (c) n = 4, (d) n = 6, and (e) n = 8.

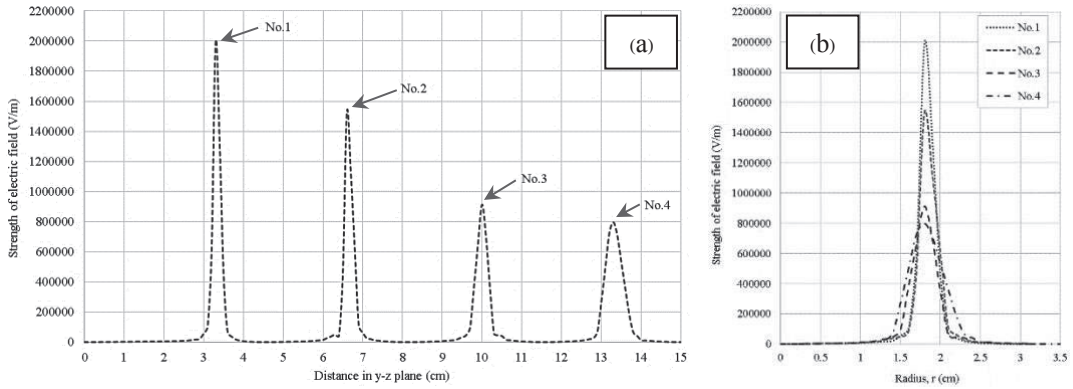

Figure 3 Distribution of electric field strength from each electrode end in y-z plane when n = 8 : (a) various electrode positions, (b) combination of electric field shape

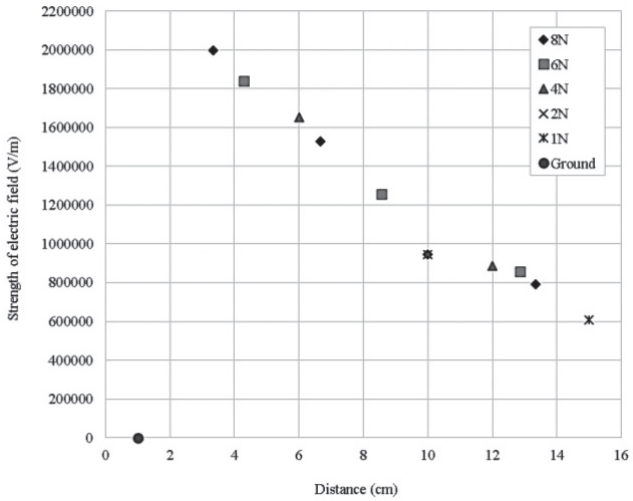

Figure 4 Distribution of electric field from electrode ends.

Figure 2 shows the maximum strength of electric fields (y-z plane) from each electrode ends. It is found that the maximum strength of electric field varies according to the number of electrode applied. Moreover, the maximum strength occurs in position of the electrodes where are nearest the ground wires. Therefore, it can be pronounced that the strength of electric field depends on the distance between electrode and ground wires. For example, applying an electrode gives the lowest strength, as shown in Figure 2(a). However, it is found from Figure 2(e) which plots the peak strength from each electrode that the strength rapidly decreases and is inversely varies with the distance square. Furthermore, each field does not influence the other fields. Therefore, electric force individually performs on the air elements.

Distribution in y-z plane of electric fields computed through Maxwell equations shows in Figure 3. It is found Figure 3(a) that the strength of electric field rapidly decreases from the center of electrode. Figure 3(b) shows the distribution of electric field from an electrode end. The electric field occupies in a certain region. Therefore, influence of electric force onto air performs only in region near the electrode end.

Figure 4 shows the distribution of electric field from electrode ends and plots at the electrode positions. The maximum strength is at the electrode position. Due to distance between electrode and ground positions, it causes distribution not to be symmetry. The strength much more decreases when it is further away from electrode end.

3.2 Velocity field

Figure 5 and 6 show the distribution of electric field and velocity field induced by electric force. High velocity field

occurs in the electrode ends which provide the high strength of electric field. In addition, high velocity occurs in where the electrode near ground wire, as shown in Figure 6. This is because the maximum strength of electric field occurs in this region. By applying more number of electrode wires, it conducts the electrode is much closer the ground wire, resulting in higher air velocity, and more violent flow motion.

Figure 7 and 8 shows the electric field distribution and velocity field (in x-z plane) when 8 electrodes are installed at elevation E_z = 2 cm. The figures show that the location of circulating flow varies according to electrode locations. By considering the location of packed bed as target position (x = 30 to 33.75 cm), installing the electrodes at E_x = 33.75 cm conduct the circulating flow occurs in front of the packed bed. resulting higher drying rate as shown in research done by Nukan et al [10].

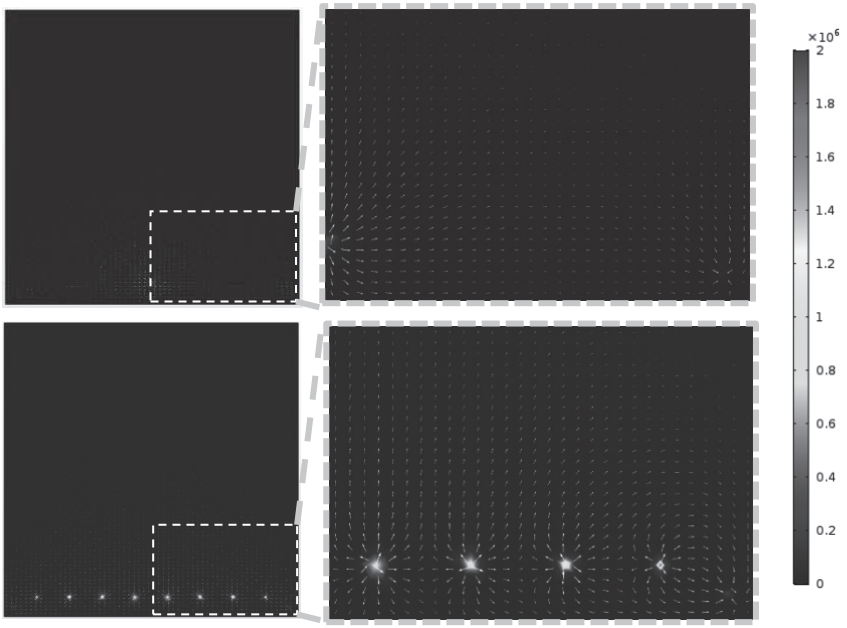

Figure 5 Electric field (V/m) distribution between one and eight electrodes.

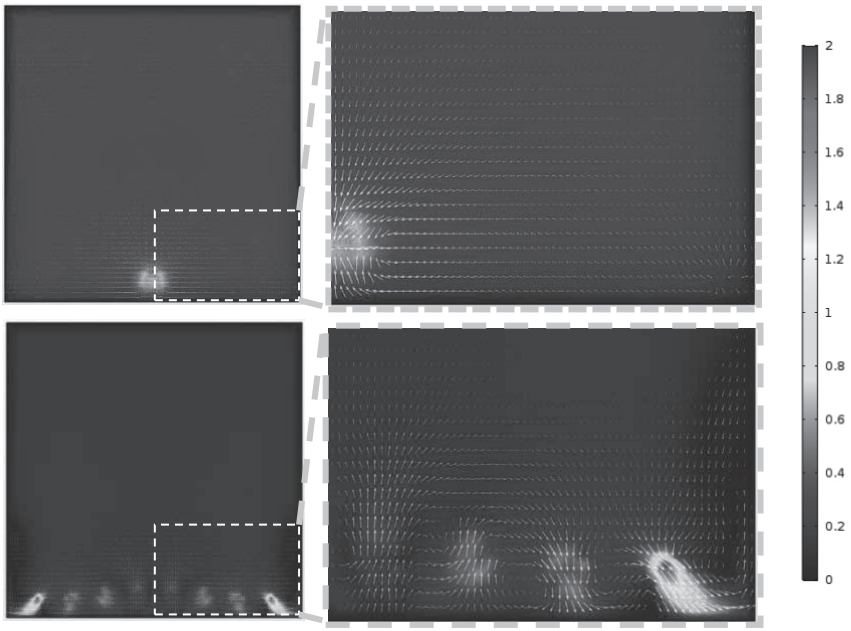

Figure 6 Velocity field induced (m/s) by electric force between one and eight electrodes.

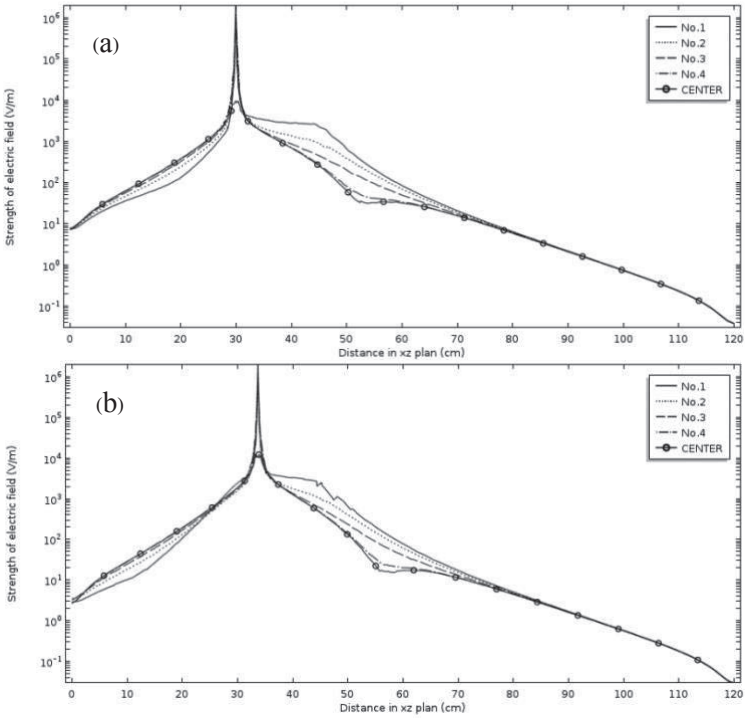

Figure 7 Distribution of electric field (V/m) in various x-z plane: (a) Ex = 30 cm, and (b) Ex = 33.75 cm.

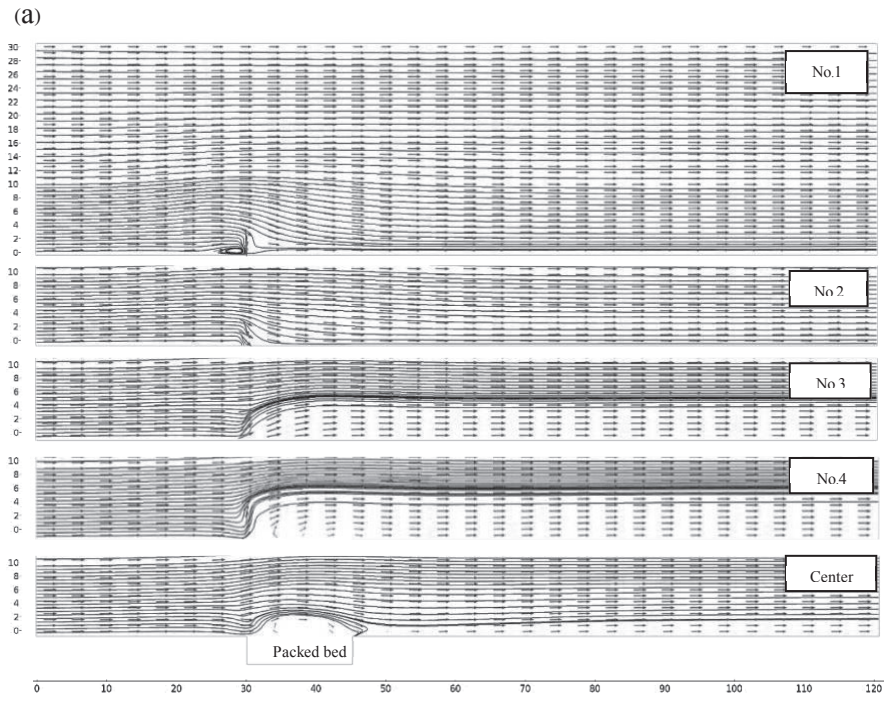

(b)

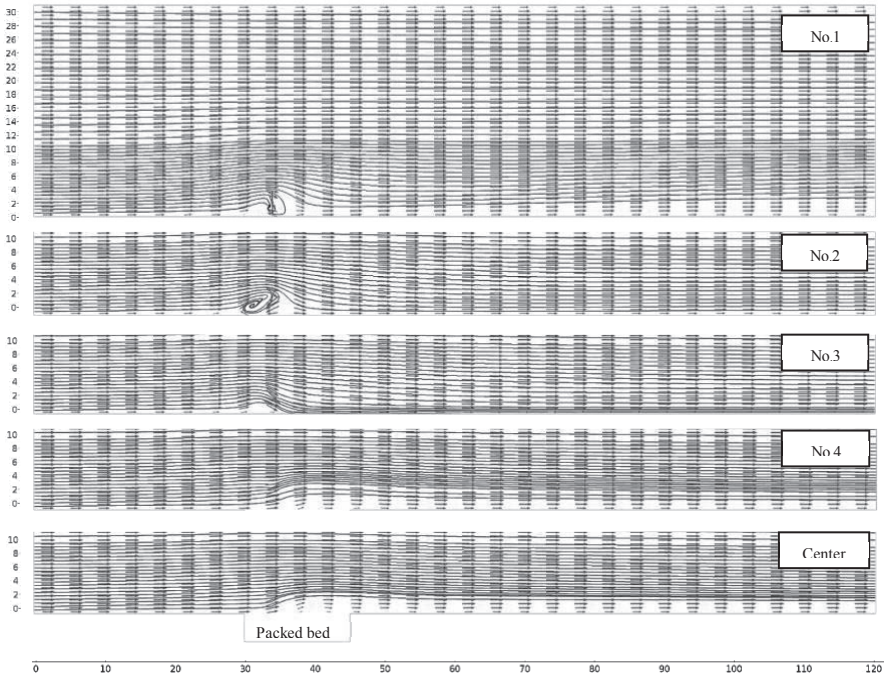

Figure 8 Velocity field (m/s) in various x-z plane: (a) E_x = 30 cm, and (b) E_x = 33.75 cm.

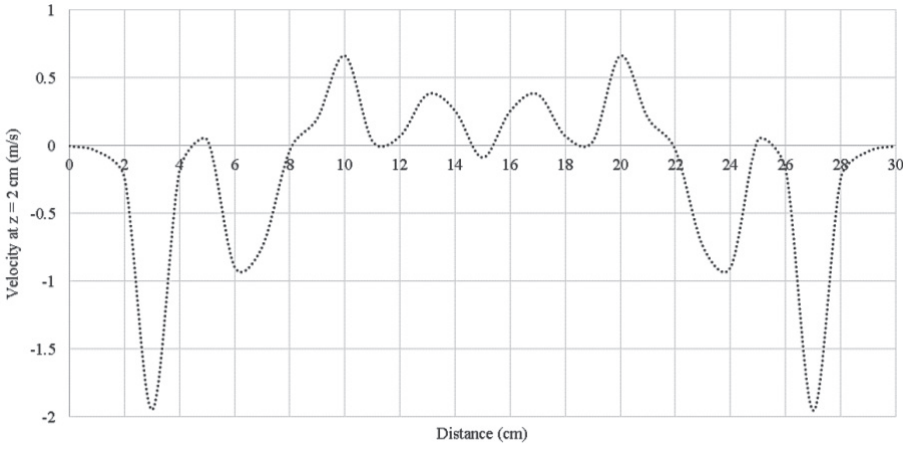

Figure 8 Air velocity (m/s) in spanwise direction

Figure 8 shows that air velocity in y-z plane depends on the electrode position. The high velocity occurs at the electrode ends close to the ground. Therefore, increasing the number of electrode causes the distance between electrode and ground wires to be shorter, resulting in higher swirling flow.

4. Remarking conclusions

The research can be summarized as follows.

- High electric field strength occurs around the electrode ends and it steeply decreases by following the distance far away from the center of electrode ($E \propto 1/r^5$). Additionally, the electric field does not much influence nearby electrodes. By plotting the peak from electrode end, it is found that the peak E is proportional to $1//d^2$. The maximum peak occurs at the electrode installed nearest the ground wire.
- Position of the high airflow velocity is consistent with the position of the peak electric field. Therefore, the rotating flow is highly strong around the electrode near the walls. In addition, electrode normal to flow direction and ground parallel to flow direction can induce the rotating flow in the plane normal to flow direction.
- Adjusting the electrode position closer to the center of ground causes the whole airflow velocity to become wider and stronger on the surface of packed bed.

5. Acknowledgement

This work is supported by faculty of engineering, Thammasat University, Rangsit center.

6. References

[1] Chaktranond C., and Rattanadecho P. Analysis of heat and mass transfer enhancement in porous material subjected to electric fields (Effects of particle sizes and layered arrangement). Experimental Thermal and Fluid Science. 2010; 34 (8): 1049-1056.

[2] Wang W., Yang L., Wu K., Lin C., Huo P., Liu S., Huang D., and Lin M. Regulation- controlling of boundary layer by multi-wire-to-cylinder negative corona discharge. Applied Thermal Engineering. 2017; 119: 438-448.

[3] Lai F.C., and Zhang J. Effect of emitting electrode number on the performance of EHD gas pump in a rectangular channel. Journal of Electrostatics. 2011; 69: 486-493.

[4] Lee J.R., and Lau E.V. Effects of relative humidity in the convective heat transfer over flat surface using ionic wind. Applied Thermal Engineering. 2017; 114: 554-560.

[5] Lai F.C., and Lai K.W. EHD-Enhanced drying with wire electrode. Drying Technology. 2002; 20(7): 1393-1405.

[6] Lai F.C., and Wang C.C. EHD-enhanced water evaporation from partially wetted glass beads with auxiliary heating from below. Drying Technology. 2009; 27: 1199-1204.

[7] Ahmedou A.O., Rouaud O., and Havet M. Assessment of the electrohydrodynamic drying process. Food Bioprocess Technology. 2009; 2: 240-247.

[8] Sanewong Na Ayuttaya S., Chaktranond C., and Rattanadecho P. Numerical analysis of electric force influence on heat transfer in a channel flow (Theory based on saturated porous medium approach). Journal of Heat and Mass Transfer. 2013; 64: 361-374.

[9] Heidarinejad G., and Babaei R. Numerical investigation of electrohydrodynamics (EHD) enhanced water evaporation using large eddy simulation turbulent model. Journal of Electrostatics. 2015; 77: 76-87.

[10] Chaktranond C., Nuknan N., and Rattanadecho P. Investigation of spiral flow generation using electrohydrodynamics for enhancement of hot-Air drying efficiency. Journal of Science and Technology. 2014; 22: 906-913.